

**Agnieszka Martyla<sup>1\*</sup>, Maciej Kopczyk<sup>1</sup>, Monika Osińska-Broniarz<sup>1</sup> Piotr Marciniak<sup>2</sup>  
Agnieszka Czapiak<sup>3</sup>, Łukasz Majchrzycki<sup>3</sup>, Robert Przekop<sup>3</sup>**

<sup>1</sup> Institute of Non-Ferrous Metals, Division in Poznan, Central Laboratory of Batteries and Cells, ul. Forteczna 12, 61-362 Poznań, Poland

<sup>2</sup> Poznan Science and Technology Park of Adam Mickiewicz University Foundation, ul. Rubież 46, 61-612 Poznań, Poland

<sup>3</sup> Centre of Advanced Technologies Adam Mickiewicz University, ul. Umultowska 89c, 61-614 Poznań, Poland

\*Corresponding author. E-mail: agnieszka.martyla@clao.poznan.pl

Received (Otrzymano) 22.06.2015

## NEW METHOD OF OBTAINING CuO-SnO<sub>2</sub> NANOCOMPOSITE

In this paper, we proposed a new synthesis method of a CuO-SnO<sub>2</sub> composite based on the sol-gel technique and tin(IV) acetate as the precursor. In addition, for the first time we used a combination of high-energy homogenization and spray drying. The aim of the study was to obtain a nano-composite with a high Cu content. The system properties were investigated using XRD, TGA, TEM and SEM-EDS techniques. The obtained composite material contains an amorphous gel of tin(IV) hydroxide and crystalline copper(II) acetate. The presented method of synthesis allows for obtaining nano-composite particle sizes less than 50 nm, and a CuO-SnO<sub>2</sub> nano-composite fraction with a particle size less than 5 nm. The small size of particles should result in high activity of the system.

**Keywords:** sol-gel, composite, spray drying, SnO<sub>2</sub>, CuO, Cu

## NOWA METODA OTRZYMYWANIA NANOKOMPOZYTOWEGO UKŁADU CuO-SnO<sub>2</sub>

W niniejszej pracy proponujemy nową metodę otrzymywania układu CuO-SnO<sub>2</sub>, wykorzystującą technikę zol-żel i octan cyny(IV) jako prekursor SnO<sub>2</sub>. Ponadto, po raz pierwszy zastosowano połączenie techniki wysokoenergetycznej homogenizacji i suszenia rozpyłowego. Celem pracy było otrzymanie układu nanokompozytowego o wysokiej zawartości Cu. Otrzymane układy zostały poddane charakterystyce za pomocą technik XRD, TGA, TEM oraz SEM-EDS. Kompozyty zawierają amorficzny żel wodorotlenku cyny(IV) oraz krystaliczny octan cyny(II). Dzięki zastosowaniu wspomnianych technik udało się otrzymać cząsteczki o rozmiarach poniżej 50 nm, jak również pewną frakcję nanokompozytu CuO-SnO<sub>2</sub> o rozmiarach poniżej 5 nm. Małe rozmiary cząstek powinny wpływać na wysoką aktywność takiego układu.

**Słowa kluczowe:** zol-żel, kompozyt, suszenie rozpyłowe, SnO<sub>2</sub>, CuO, Cu

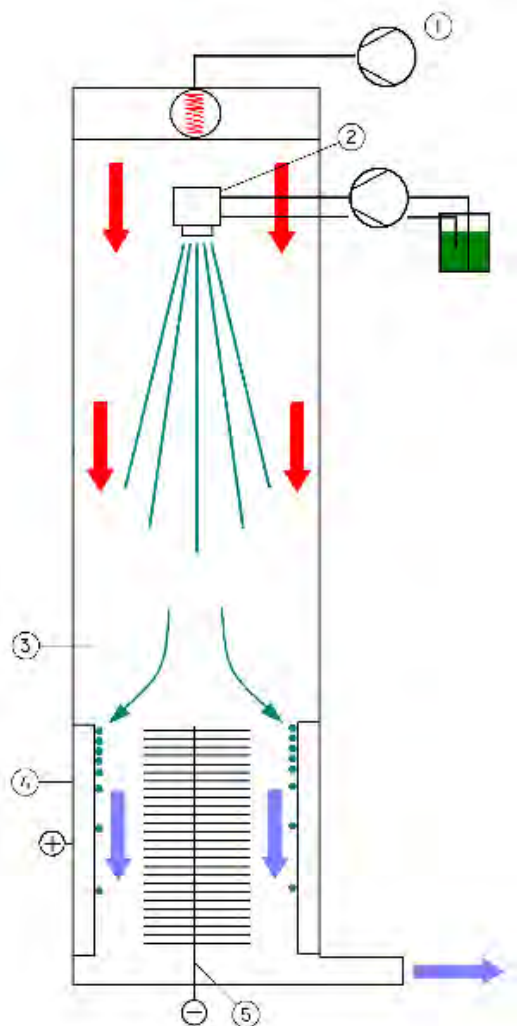
## INTRODUCTION

CuO-SnO<sub>2</sub> composites are used as electrode material [1] and in semiconductor sensors of toxic and combustible gas [2]. Much attention has been paid to research work to optimize the sensor by modeling the SnO<sub>2</sub> structure [3, 4]. Previous studies confirm that the use of copper oxide improves sensor performance characteristics and sensitivity [5-8]. Semiconducting tin oxide thin films with nano-catalysts, overlayers, clusters etc. [9] are known to exhibit enhanced sensitivity, better selectivity and fast response speeds to various reducing gases including H<sub>2</sub>S. An SnO<sub>2</sub> sensor is invariably anion deficient and oxygen vacancies are mainly responsible for making free electrons available for the conduction process [10]. In addition, the surface morphology of the sensing layer is also important for creating a sensor with enhanced response characteristics, which in turn depends on the growth kinetics [11]. CuO-doped SnO<sub>2</sub> thick films are found to exhibit extraordinary

sensing characteristics for H<sub>2</sub>S. However, the response time is in the range of 5~15 min [12, 13-15]. Some of the extensively investigated sensor structures for H<sub>2</sub>S gas detection include mixed CuO-SnO<sub>2</sub> powders [16], Cu-SnO<sub>2</sub> bi-layers [17], CuO-SnO<sub>2</sub> hetero-structures as well as others [8, 18]. The processing conditions have been noted to have a significant influence on the sensing response characteristics. It has been shown that the introduction of CuO nano-particles on a SnO<sub>2</sub> thin film surface advantageously leads to fast recovery [19]. However, a systematic study exploring new preparation methods and the influence of a CuO catalyst in enhancing the H<sub>2</sub>S gas detection capability of SnO<sub>2</sub> thin films has yet to be carried out. It is difficult to pinpoint the exact physical mechanism, however, sensor resistance is expected to increase if oxygen is somehow adsorbed onto the SnO<sub>2</sub> film surface. Furthermore, the presence of the copper catalyst is expected to introduce the spill-

over phenomenon besides the creation of a barrier at the catalyst-sensing layer interface, leading to influencing the sensor resistance [11].

This study presents a new synthesis method of a CuO-SnO<sub>2</sub> nano-composite system possessing a homogenous structure in nanoscale. We described a method for obtaining that system using the sol-gel technique and tin (IV) acetate as the SnO<sub>2</sub> precursor, high-energy homogenization and spray drying. The obtained systems were characterized by XRD, TGA, TEM and SEM-EDS techniques. Thanks to the novel homogenization method, a great speed of formulation can be achieved, which is less time consuming and more efficient. Spray drying is a continuous process to transform liquids (solutions, emulsions, slurries, pastes or even melts) into micron size particles with adjustable distribution, shape, porosity, density and chemical composition. Spray drying is widely applied in materials, chemical, food and pharmaceutical industries. In the presented work the Büchi spray drying system was used (Fig. 1).



1. Drying gas in, 2. Nozzle, 3. Drying chamber, 4. Collecting electrode, 5. Grounded electrode

Fig. 1. Diagram of spray drying process

Rys. 1. Schemat procesu suszzenia rozpyłowego

## EXPERIMENTAL PROCEDURE

20 ml of a tin(IV) acetate solution (containing 60 mg of tin(IV) acetate in 1 ml isopropanol) was added to a 40 ml water solution of copper (I) acetate (containing 50 mg of copper (I) acetate in 1 ml) and 1 ml propyl glycol. The solution was mixed with a Heidolph Silent Crusher M homogenizer for 10 minutes at 26.000 rpm. Then the suspension was filtered through a 200 nm pore filter. The filtrate was dried using a Büchi Nano Spray Dryer B-90. The drying parameters were as follows: pressure 56 hPa, air temperature 90°C, air flow 150 l/min, drying head 5.5 µm and head opening 100%.

## PHYSICOCHEMICAL CHARACTERISTICS

Phase identification was performed using an  $\mu$ XRPD. A small amount of sample was placed in a thin-walled glass mark-tube (Hilgenberg GmbH), mounted on the X-ray diffractometer and centered with the optical microscope. The Oxford Diffraction New Xcalibur diffractometer using MoK $\alpha$  radiation ( $\lambda = 0.71073 \text{ \AA}$ ), equipped with a graphite monochromator and a CCD detector (EosS2), was employed for data collection. A 0.3 mm pinhole collimator was used and the detector was set at 100 mm from the sample. The exposure time was fixed to 300 seconds per scan and the images were collected with a 300 degree phi rotation. Data collection and reduction were performed with CrysAlisPro software [20].

Surface imaging was performed with Transmission Electron Microscopy (TEM) - JOEL JEM 1200 EX and Scanning Electron Microscopy SEM - EDS. Thermal Analysis was carried out using a Thermobalance TG 209 F1 Libra Netzsch.

## RESULTS AND DISCUSSION

The specific properties of the nanoparticles results in numerous difficulties during their synthesis. Strong interactions and agglomeration propensity demand using high dilution in conducting the synthesis. The surfactants and complexing agent cause many problems to separate them from the nanoparticles and sometimes it is not even possible.

The presented strategy of nano-composite oxide particle production is based on separation and elimination of particles not meeting the set diameter criteria. Thanks to high energy homogenization, the amount of particles smaller than the 200 nm size is much greater than in the case of systems obtained by traditional methods, either by participation or the sol-gel method [21, 22].

XRD analysis was carried out after thermal treatment of the resulting materials (Fig. 2).

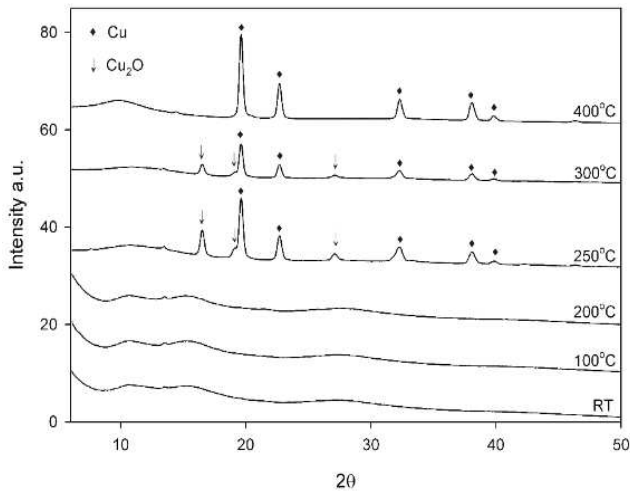


Fig. 2. Diffractometric patterns of CuO-SnO<sub>2</sub> composite after thermal treatment

Rys. 2. Dyfraktogramy kompozytu CuO-SnO<sub>2</sub> po obróbce temperaturowej

The produced CuO-SnO<sub>2</sub> composite shows no XRD diffraction pattern at room temperature, indicating the amorphous and nanostructured composition of the obtained material. Thermal treatment at temperatures not exceeding 200°C does not cause structural changes. Reflexes resulting from the Cu<sub>2</sub>O and Cu crystallites start to appear after exposure to temperatures above 200°C. At temperatures over 400°C, only reflexes attributed to Cu can be observed. This is in accordance with the thermal decomposition scheme of copper (II) acetate [23] (Fig. 3). In “normal” conditions the final decomposition product is CuO. In the case of the CuO-SnO<sub>2</sub> composite, only metallic copper reflexes can be observed. This is an additional indicator of the nano-metric size of the formed structures.

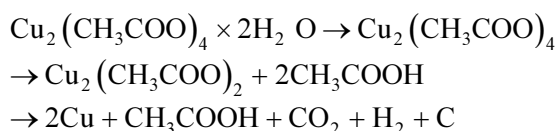


Fig. 3. Scheme of thermal decomposition of copper acetate(II)

Rys. 3. Schemat rozkładu termicznego octanu miedzi(II)

The tin content was measured using an SEM-EDS (Fig. 4). The tin content at approximately 12.5% suggests that its major part was separated during filtration with the 0.2 μm filter. The results of the SEM-EDS measurements prove the high uniformity of the produced nano-composite. The agglomerate size does not exceed 3 μm and most (above 80%) is below 1 μm.

In order to confirm the nano-composite particle size, TEM observations were conducted. The microphotographs show the presence of particles even smaller than 5 nm (Fig. 5).

The thermal analysis of the CuO-SnO<sub>2</sub> system is presented in Figure 6.

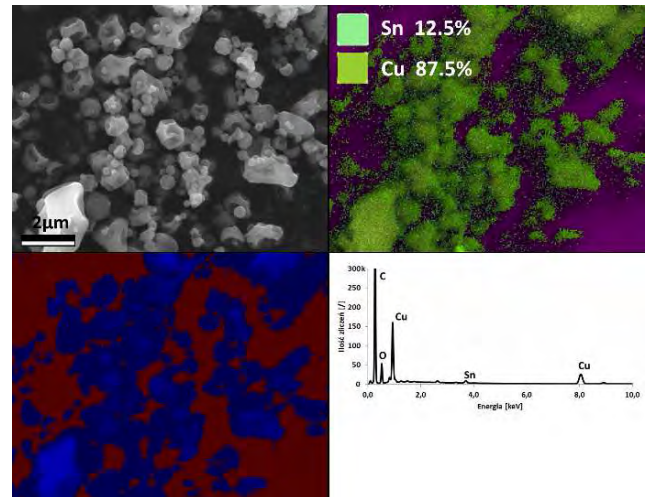


Fig. 4. SEM-EDS analysis of CuO-SnO<sub>2</sub> composite

Rys. 4. Analiza SEM-EDS kompozytu CuO-SnO<sub>2</sub>

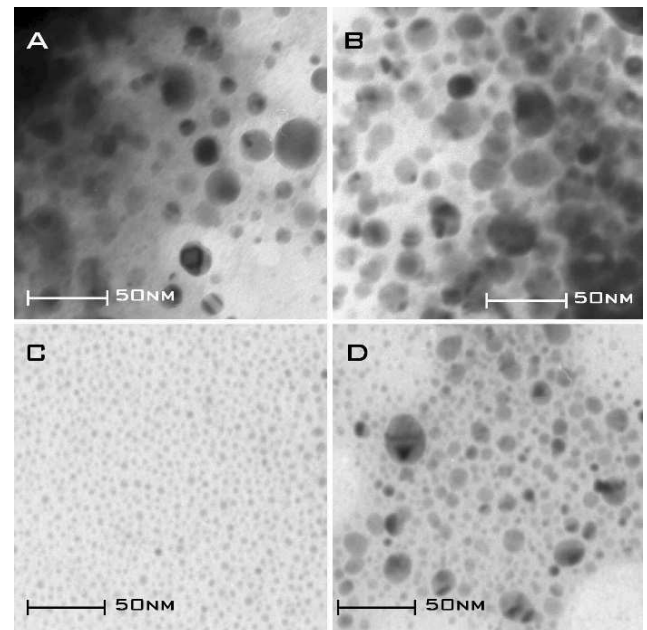


Fig. 5. TEM micrograph of CuO-SnO<sub>2</sub> composite

Rys. 5. Zdjęcia TEM kompozytu CuO-SnO<sub>2</sub>

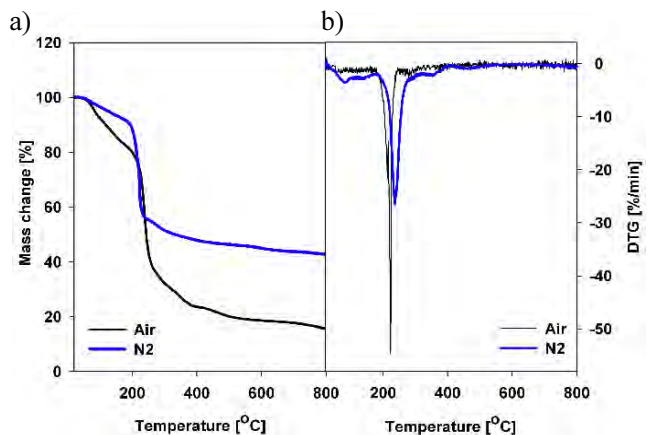


Fig. 6. Thermal decomposition of CuO-SnO<sub>2</sub> composite: a) TG, b) DTG

Rys. 6. Rozkład termiczny kompozytu CuO-SnO<sub>2</sub>: a) TG, b) DTG

The thermal decomposition of the nano-composite proceeds at a temperature close to the copper(II) and tin(IV) acetate decomposition temperature. The first section of the mass loss curve effect presents hydration water removal, which occurs below 200°C. The next effect is related to the thermal decompositions of acetates and production of water and carbon dioxide. Metallic copper and tin(IV) oxide is the final product of the system decompositions.

## CONCLUSIONS

The presented method of synthesizing nanocomposites can be an alternative route of producing nanoparticles possessing a complex chemical composition. The size of the obtained nanoparticles is in the range from 3 to 25 nm. The amorphous composite contains 87% Cu and 12.5% Sn. Thermal decomposition results in a material consisting of metallic copper and an SnO<sub>2</sub> phase that shows no XRD reflexes.

## Acknowledgements

*The study was financially supported by statutory activity of the IMN Division in Poznan CLAiO.*

## REFERENCES

- [1] Martyla A., Majchrzycki L., Marciniak P., Sztorch B., Kopczyk M., Przekop R., Otrzymywanie cienkich warstw SnO<sub>2</sub> dla fotowoltaicznych materiałów elektrodowych przy użyciu techniki zol-żel, *Chemik* 2013, 67 (12), 11-15.
- [2] Elvers B., Hawkins S., Ravenscroft M., Schulz G. (Eds.), *Ullmann Encyclopedia of Industrial Chemistry*, vol. A13VCH, Weinheim 1989, 467.
- [3] Kim S.T., Park M.S., Kim H.M., Systematic approach for the evaluation of the optimal fabrication conditions of a H<sub>2</sub>S gas sensor with Taguchi method, *Sensors and Actuators B: Chemical* 2004, 102, 253-260.
- [4] Ionescu R., Hoel A., Granqvist C.G., Llobet E., Heszler P., Low-level detection of ethanol and H<sub>2</sub>S with temperature-modulated WO<sub>3</sub> nanoparticle gas sensors, *Sensors and Actuators B: Chemical* 2005, 104, 132-139.
- [5] Sberveglieri G., Gropelli S., Nelli P., Pergo C., Valdre G., Camanzi A., Detection of sub-ppm H<sub>2</sub>S concentrations by means of SnO<sub>2</sub>(Pt) thin films grown by RGTO technique, *Sensors and Actuators B: Chemical* 1993, 86, 15-16.
- [6] Maekawa T., Tamaki J., Miura N., Yamazoe N., Sensing behavior of CuO-loaded SnO<sub>2</sub> element for H<sub>2</sub>S detection, *Chemical Letter* 1991, 4, 575.
- [7] Manorama S., Devi G.S., Rao V.J., Hydrogen sulfide sensor based on tin oxide deposited by spray pyrolysis and microwave plasma chemical vapor deposition, *Applied Physical Letter* 1994, 64, 3163-3165.
- [8] Chowdhuri A., Gupta V., Sreenivas K., Kumar R., Mozumdar S., Patanjali P.K., Response speed of SnO<sub>2</sub>-based H<sub>2</sub>S gas sensors with CuO nanoparticles, *Applied Physical Letter* 2004, 84, 1180-1183.
- [9] Chowdhuri A., Sharma P., Gupta V., Sreenivas K., Rao K.V., H<sub>2</sub>S gas sensing mechanism of SnO<sub>2</sub> films with ultrathin CuO dotted islands, *Journal of Applied Physics* 2002, 92(4), 2172-2180.
- [10] Haridas D., Sreenivas K., Gupta V., Improved response characteristics of SnO<sub>2</sub> thin film loaded with nanoscale catalysts for LPG detection, *Sensors and Actuators B: Chemical* 2008, 133, 270-275.
- [11] Chowdhuri A., Haridas D., Sreenivas K., Gupta V., Mechanism of trace level H<sub>2</sub>S gas sensing using of sputtered SnO<sub>2</sub> thin films with CuO catalytic overlayer, *International Journal Smart Sensing and Intelligent Systems* 2009, 2(4), 540-548.
- [12] Yamazoe N., Tamaki J., Miura N., Role of hetero-junctions in oxide semiconductor gas sensors, *Materials Science and Engineering: B* 1996, 41, 178-181.
- [13] Tamaki J., Maekawa T., Miura N., Yamazoe N., CuO-SnO<sub>2</sub> element for highly sensitive and selective detection of H<sub>2</sub>S, *Sensors and Actuators B: Chemical* 1992, 9(3), 197-203.
- [14] Tamaki J., Shimanoe K., Yamada Y., Yamamoto Y., Miura N., Yamazoe N., Dilute hydrogen sulfide sensing properties of CuO-SnO<sub>2</sub> thin film prepared by low-pressure evaporation method, *Sensors and Actuators B: Chemical* 1998, 49, 121-125.
- [15] Maekawa T., Tamaki J., Miura N., Yamazoe N., Sensing behavior of CuO-loaded SnO<sub>2</sub> element for H<sub>2</sub>S detection, *Chemical Letter* 1991, 20, 575-578.
- [16] Lantto V., Romppainen P., Rantala T. S., Leppavuori S., Equilibrium and non-equilibrium conductance response of sintered SnO<sub>2</sub> samples to H<sub>2</sub>S, *Sensors and Actuators B: Chemical* 1991, 5, 451-455.
- [17] Jianping L., Yue W., Xiaoguang G., Quing M., Li W., Jinghong H., H<sub>2</sub>S sensing properties of the SnO<sub>2</sub>-based thin films, *Sensors and Actuators B: Chemical* 2000, 65, 111-113.
- [18] Vasiliev R.B., Romyantseva M.N., Podguzova S.E., Ryzhikov A.S., Ryabova L.I., Gaskov A.M., Effect of interdiffusion on electrical and gas sensor properties of CuO/SnO<sub>2</sub> heterostructure, *Materials Science and Engineering: B* 1991, 57, 241-246.
- [19] Chowdhuri A., Gupta V., Sreenivas K., Kumar R., Mozumdar S., Patanjali P. K., Response speed of SnO<sub>2</sub> - based H<sub>2</sub>S gas sensors with CuO nanoparticles, *Applied Physical Letter* 2004, 84, 1180-1182.
- [20] Agilent Technologies, Program CrysAlisPro, ver.171.37.31, Yarnton, Oxfordshire, England 2014.
- [21] Martyla A., Kopczyk M., Marciniak P., Przekop R., Platinum(0)-1,3-divinyl-1,1,3,3-tetramethyldisiloxane complex as a Pt source for Pt/SnO<sub>2</sub> catalyst, *J. Nanomaterials* 2014, Article ID 275197.
- [22] Martyla A., Kopczyk M., Marciniak P., Przekop R., One-pot method of synthesis of Pt/SnO<sub>2</sub> system and its electrocatalytic activity, *Chem. Central. Journal* 2014, 8, 49.
- [23] Judd M.D., Plunkett B.A., Pope M.I., The thermal decomposition of calcium, sodium, silver and copper (II) acetates, *Journal of Thermal Analysis* 1974, 6, 555-563.